

A Software Signal Simulation of Low Earth Orbit Satellites for Investigative Analysis

by

Samuel McDougal

A thesis submitted to the Graduate Faculty of
Auburn University
in partial fulfillment of the
requirements for the Degree of
Master of Science

Auburn, Alabama
Sometime Spring 2023

Keywords: LEO Satellites, USRP, Navigation, Signals of Opportunity

Copyright 2023 by Samuel McDougal

Approved by

Scott Martin
David Bevly
Brendon Allen

Abstract

Place the text of the abstract here. Headings come automatically.

Acknowledgments

acknowledgments

Table of Contents

Abstract	ii
Acknowledgments	iii
1 Introduction	1
1.1 Motivation	1
1.2 Prior Work	1
1.3 Contributions	3
1.4 Thesis Outline	3
2 Background	4
2.1 Satellite Orbit Zones	4
2.2 Low Earth Orbit Satellites	6
2.2.1 Current LEO Constellations	6
2.3 Channel Access Methods	7
2.3.1 Time Division Multiple Access	7
2.3.2 Code Division Multiple Access	8
2.3.3 Frequency Division Multiple Access	9
2.4 Modulation	9
2.4.1 Binary Phase Shift Keying	10
2.4.2 Quadrature Phase Shift Keying	11
2.5 Satellite Based Navigation	11

3	Simulation Tool	13
3.1	Simulator Overview	13
3.2	Simulation Settings	14
3.3	Measurement Simulation	15
3.4	Signal Simulation	18
3.5	Receiver	21
4	Testing Setup and Positioning Techniques	22
4.1	Doppler Based Positioning	22
4.2	Pseudorange Based Positioning	25
5	Results	27
5.1	Static Clean Data	27
5.1.1	Doppler Positioning	27
5.1.2	Pseudorange Based Positioning	29
5.2	Static Clean Data Played Through USRP	29
5.2.1	Doppler Positioning	29
5.2.2	Pseudorange Based Positioning	29
5.3	Static Dirty Data	29
5.3.1	Doppler Positioning	29
5.3.2	Pseudorange Based Positioning	29
5.4	Dynamic Clean Data	29
5.5	Dynamic Clean Data Played Through USRP	29
5.6	Dynamic Dirty Data	29
6	Conclusions and Future Work	30
	Bibliography	31

Appendices	34
----------------------	----

List of Figures

2.1	Visual Representation Orbit Zones	5
2.2	Visual Representation of TDMA Signal	8
2.3	Amplitude Shift Keying Visualization [1]	9
2.4	Amplitude Shift Keying Visualization [2]	10
2.5	Binary Phase Shift Keying Visualization [3]	10
2.6	Quadrature Phase Shift Keying Visualization [3]	11
2.7	Visual Depiction of Trilateration	12
3.1	Overall Simulation Diagram	13
3.2	Measurement Generation Block Diagram	16
3.3	Propagated Satellites from SGP4	17
3.4	Signal Simulation Block Diagram	19
3.5	Signal Generation Block Diagram	20
5.1	Position Estimate from Batched Doppler Measurements	28
5.2	RMS Error of Batched Doppler Estimates	28

List of Tables

Chapter 1

Introduction

1.1 Motivation

Low Earth orbit (LEO) satellites for navigation have gained interest as an alternative source of position, navigation and timing (PNT) to GNSS due to GNSS being susceptible to interferences such as jamming, spoofing, and multipath. Many current LEO satellites are not designed for navigation, however their signals have been exploited for opportunistic navigation. Many of these constellations have data messages that are unknown to the user which makes receiver design difficult. While there are a few high fidelity LEO simulators on the market, they can be expensive. These tools allow for testing of signal types before satellites are launched and signals can be replicated with prior knowledge of the signal. The development of a signal simulation tool that allows for testing of different signal types, satellite constellations, and receiver patterns is a necessary tool for developing software and hardware receivers for LEO satellites.

1.2 Prior Work

There are recent studies in positioning techniques with the growing interest in finding navigation possibilities with LEO satellites. Currently, global navigation satellite systems (GNSSs) are an integral part of modern society. Whether it is directions to the grocery store, land surveying, or autonomous vehicles, the knowledge of where something is and where it is supposed to

go is important. Current GNSSs, such as Global Positioning System (GPS), use radio frequencies (RF) to determine position and velocity solutions. Methods for calculating positions and velocities from GPS satellites can be found in [4].

The flexibility of a simulation tool is crucial. It saves time, money, and resources when testing different scenarios. One of the biggest advantages to this simulation tool is the ability to interchange different pieces quickly and efficiently. Whether it is the constellation type, data message, or signal structure, changes can be made easily to accommodate varying test plans. Current navigation simulation tools are mainly focused on GNSSs such as [5] and [6]. One source, [7] designs a signal simulation tool for “Rapid Testing of Interference Mitigation Techniques” for GPS. In his thesis, Powell outlines structures for creating a low cost signal simulation tool that can be used to test different scenarios. He begins by generating a file of simulation settings. This is followed by a scenario simulation where satellites are propagated, measurements are generated, and the navigation message populated. Next the signal is generated for the satellites in view and the data is stored in a bin file. GNSS signal simulators can also be used to test software defined receivers (SDRs). Powell validates his simulation by comparing the generated signal performance to the performance of a hardware gps receiver and examining the position, velocity, carrier to noise ratio, and Doppler frequencies. Powell found that the simulator described in his thesis was capable of producing realistic single and multi antenna signals.

One of the main areas of research for LEO satellites is using the Doppler frequency measurements from the LEO satellites in order to gain a navigation solution [8] [9]. Doppler positioning has been used in GNSS [10], and was even the precursor to GPS [11]. The Transit satellite system was initially used for US naval ships to gain a rough position. In [12], Thompson uses a double differenced Doppler technique to position a moving rover with LEO satellites using angle of arrival (AOA) estimates to remove the need of satellite state knowledge. The Argos satellite system uses Doppler measurements for animal tracking [13]

Another area of research with LEO satellites is to use their measurements and colaberate with IMUs for opportunistic navigation[14] and [15]. In [16], the Orbcomm constellation is used to to aid an inertial navigation system (INS) in a tightly-coupled fashion. Here they used

the LEO satellite Doppler measurements and TLE files to estimate the position of a moving UAV without GNSS signals. For the experiment, the UAV was without GPS and had 2 Orbcomm satellites. They claim that this navigation framework lowered the UAV final position error by 72 percent when compared to solely using the IMU.

One possibility is to deploy a new constellation in LEO specifically for navigation [17].

A LEO satellite signal simulator can be useful for testing different signal types, constellation geometries, and possible errors. The results of a simulation are only as good as the simulator itself. While high end signal simulators exist, they can be expensive and require technical prowess to operate. A low cost version can be valuable and still operate at a high level of fidelity with more ease of use.

1.3 Contributions

This thesis will describe the process of designing a modular simulation tool for LEO satellites. The versatility of the simulator allows the user to test different scenarios. The contributions from this thesis are listed below:

- Description of LEO satellite signal simulation tool that generates realistic IQ signals to be used for current and emerging constellations
- Investigation of USRP playback and record to introduce hardware errors
- Examine possible positioning techniques for TDMA signals

1.4 Thesis Outline

In Chapter 2, the background of satellite orbits, signal types, and modulation types are discussed. In Chapter 3, the simulation tool is described in detail. Chapter 4 dives into the simulation and testing configurations used for this thesis. The results from the testing configurations are discussed in Chapter 5. Conclusions and future work are discussed in Chapter 6 followed by a list of references and an Appendix.

Chapter 2

Background

2.1 Satellite Orbit Zones

With regard to space vehicles, there are three main orbital zones. These zones are low Earth orbit (LEO), medium Earth orbit (MEO), and geosynchronous Earth orbit (GEO). These zones are differentiated by the altitude of the orbit above the surface of the Earth. Due to the nature of the orbits, the satellites in these orbital zones have varying mission types. Figure 2.1 gives a reference to each of the orbital zones.

The furthest of the orbit zones is GEO. These satellites have an orbit altitude of 35,786 kilometers. Geosynchronous orbits are positioned at this precise altitude to allow the satellite orbit period to equal the same time as the rotation of the Earth for one day. The length of the orbit lasts one sidereal day. To an observer on Earth, the satellite would appear to stay in the same place throughout the course of its life. Another form of geosynchronous orbit is the geostationary orbit. Geostationary orbits are geosynchronous orbits specifically located at the Earth's equator and have a near zero inclination angle. GEO satellites are stationed where they are due to their specific mission type. One of the best attributes a GEO satellites has is a large footprint. The large footprint, along with the twenty four hour coverage, means these satellites are great for Earth observation. This also means that fewer satellites are required to be in orbit for full Earth coverage. Many of the current GEO satellites are used for weather, climate surveying, and oceanic observations [18]. The Geostationary Operational Environmental Satellites (GOES) are the current Earth observation satellites operated by NASA and NOAA [19]. GEO satellites are not conducive for navigation. This is due to the nature of the orbit.

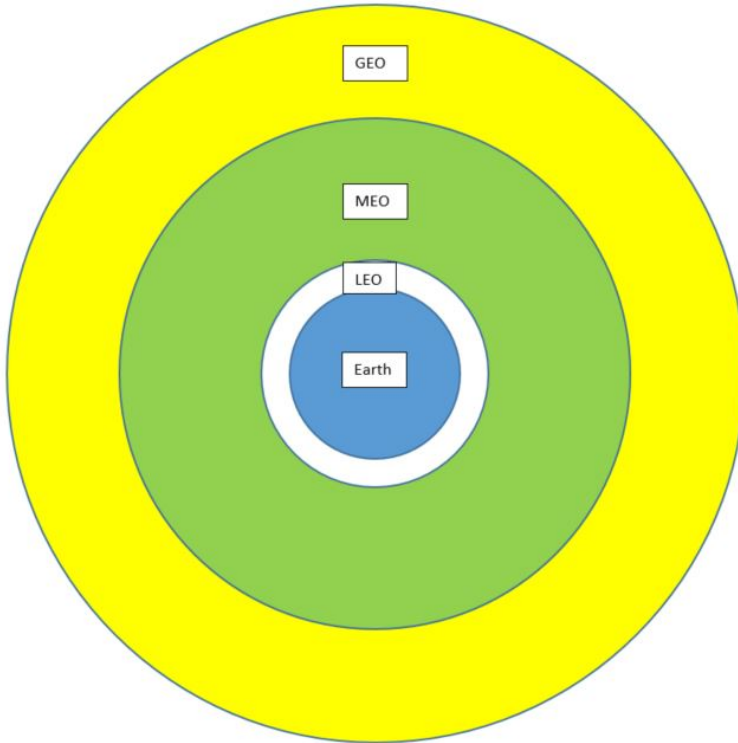


Figure 2.1: Visual Representation Orbit Zones

Since the orbit is so high, gaining a precise navigation message can be difficult due to loss of signal power and the amount of time it takes for the signal to reach Earth. Another issue with GEO satellites is the cost of launching these satellites. Launching satellites into GEO can carry a much higher price than satellites in LEO or MEO. These points were taken into consideration when GPS was first being thought about. (Maybe include an image of GEO coverage).

MEO is an orbital zone between LEO and GEO. MEO satellites have orbit altitudes between 2,000 kilometers and 35,000 kilometers. The orbit period for most MEO satellites is between 10 hours and 15 hours. Most of the satellites in MEO are navigation satellites. These constellations include GPS (USA), Galileo(European), GLONASS (Russia), and BieDou (China). Each country with GNSSs has designed them specifically for their own use. For example, GLONASS has an orbit altitude of 19,000 kilometers with satellites at specific inclination angles in order for the satellites to spend more time in view over Russia [20]. GPS occupies MEO for many reasons, one being the number of satellites needed for global coverage. While more satellites are needed in MEO for global coverage than GEO, fewer are required than in LEO. GPS satellites have an orbit period just under 12 hours. With the orbit altitude and orbit period,

24 satellites are needed for global coverage in order to have at least 4 satellites in view to gain a positioning solution. However, with an orbit period of 12 hours, the observed Doppler frequencies of the satellites are low and can lead to poor velocity estimates. Next, LEO satellites are discussed.

2.2 Low Earth Orbit Satellites

LEO satellites are different than the previously mentioned zones. LEO satellites have orbits from 300 kilometers to 1500 kilometers. With this altitude, the orbit periods for LEO satellites tend to be 60 to 90 minutes, however the amount of time that a satellite may be in view is lower. This poses issues in terms of global coverage. Satellite constellations with orbit periods on this time scale require far more satellites for full global coverage, and even more satellites for a possible navigation constellation. Reid et al says that it would take nearly 300 LEO satellites in order to provide global coverage [17]. Current LEO constellations, such as Iridium and Orbcomm, are designed for communications. The Iridium constellation uses global coverage for satellite phones, where the Orbcomm constellation uses “LEO satellites to provide worldwide geographic coverage for sending and receiving alphanumeric packages,” [21]. The data messages on these satellites are unknown as they are proprietary to the companies who sent them into space. This makes it difficult to design receivers and evaluate the navigation performance of these signals. However, a customized navigation message can be put on a similar signal.

2.2.1 Current LEO Constellations

Current LEO constellations were not designed for navigation, specifically. Most are used for satellite communications, internet, and Earth observations. Some of the major constellations in LEO are Iridium/IridiumNEXT, Orbcomm, and Starlink. The IridiumNEXT [22], which will be referred to as Iridium, is a telecommunications satellite network that comprises of 66 active satellites and 9 in-orbit spares. The 66 active satellites are grouped into 6 orbital planes with 11 satellites in each plane. These satellites are in near polar orbits which means the coverage at the poles is very high, however coverage at the equator is low. The main mission

for Iridium is to provide telecommunications with sat-phones. Orbcomm is similar to Iridium as it is a satellite communications constellation, however the physical constellation is different. Orbcomm has 48 satellites with varying inclination angles. The Starlink constellation is a satellite broadband internet provider [23]. This constellation utilizes LEO orbit in an effort reduce latency with internet signals. Instead of using typical terrestrial based techniques for internet providing, satellites are used to give coverage in places where internet may not be readily available. However to accomplish this goal, a massive constellation of satellites must be deployed. Currently, there are nearly 3,600 Starlink satellites in LEO with more planned for launch. All of these constellations have one thing in common. The original purpose of the mission was not for navigation.

2.3 Channel Access Methods

Channel access methods are ways of communicating through mediums between multiple devices. Channel access methods allow users to send information back and forth between terminals. Channel access methods are used to manage telecommunications and wireless traffic. As there are multiple users trying to use or access the same information or services, channel access methods are used to differentiate between the users and the information being passed through the mediums. Three forms of channel access methods that will be examined are time division multiple access (TDMA), code division multiple access (CDMA), and frequency division multiple access (FDMA).

2.3.1 Time Division Multiple Access

Time division multiple access signals use time to differentiate incoming signals. This results in the signal being burst-like in nature and non-continuous between received signals. The carrier frequency, however, can remain the same across all users. TDMA signals are typically used by telecommunication satellites such as Iridium. These signals are ideal for communications because as the users are separated in time, the possibility of data interference between users is low. A visual representation of a TDMA signal can be seen in figure 2.2. The burst nature of the signal can be seen in this image. The large bulk of the signal is noise, and the parts

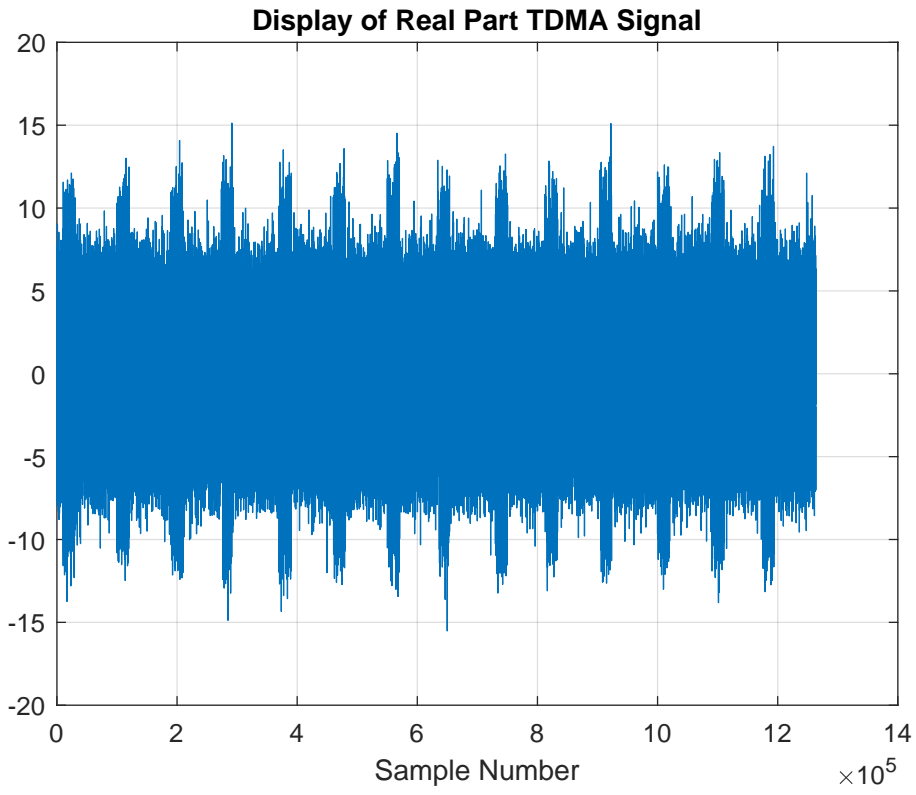


Figure 2.2: Visual Representation of TDMA Signal

extending out of the noise are the the bursts. This shows the separation of the signal accross time.

2.3.2 Code Division Multiple Access

Similar to TDMA, CDMA signals are broadcast at a single carrier frequency. However unlike TDMA, CDMA signals use deterministic binary sequence codes to differentiate signals. In the case of satellites, each satellite is given its own pseudo-random noise (PRN) sequence. These codes are designed specifically to have very low cross correlation in order to eliminate errors and deciphur different satellite's signals in the same frequency band. Cross correlation is a measure of similarity between two or more sequences. They also employ a high level of autocorrelation which is important for signal tracking [24]. Two notable GNSSs that employ CDMA signals are GPS and Galileo.

2.3.3 Frequency Division Multiple Access

Similar to CDMA, FDMA signals are continuous. However, these signals are not transmitted at the same carrier frequency. FDMA signals use different frequency bands to transmit data and information. For example, FM radio uses this technique to differentiate between radio channels such as sports talk radio and the local country music station. Similar to the radio in a car, some satellite constellations use the same idea, except each satellite transmits at a specific frequency band. For example, GLONASS uses FDMA signals for their satellites but also use a PRN code. Unlike GPS, however, they all transmit the same PRN sequence [25].

2.4 Modulation

In the world of satellite navigation and telecommunications, the term modulation refers to the process of incorporating data onto a carrier wave. This data is represented in binary form through 1's and 0's. When a signal is generated, these ones and zeros are converted into 1's and -1's for the purpose of signal modulation. Three forms of modulation include amplitude shift keying (ASK), frequency shift keying (FSK), and phase shift keying (PSK). ASK is the process of changing the amplitude of the sine wave to represent ones and zeros of binary data, FSK is the process of changing the frequency of the sine wave to represent ones and zeros of binary data, and PSK changes the phase of the signal to incorporate the data. ASK and FSK are shown in figure 2.3 and 2.4 respectively.

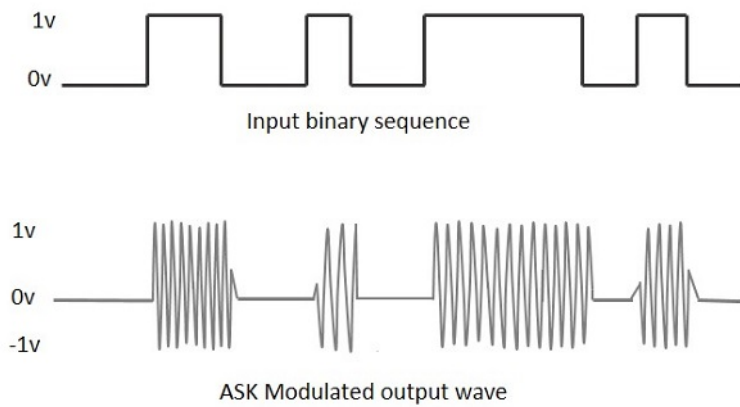


Figure 2.3: Amplitude Shift Keying Visualization [1]

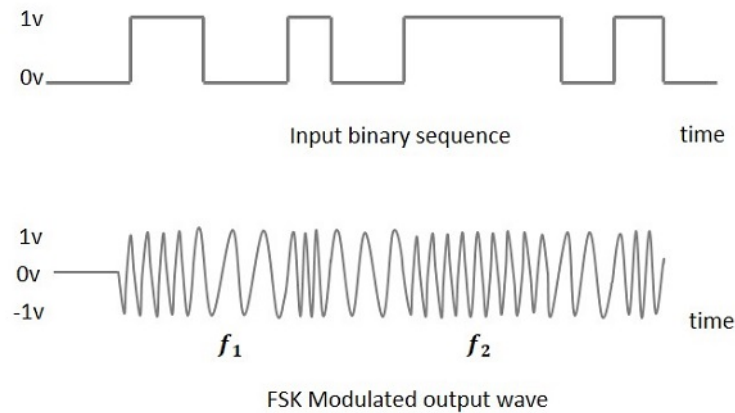


Figure 2.4: Amplitude Shift Keying Visualization [2]

Two forms of PSK are binary phase shift keying (BPSK) and quadrature phase shift keying (QPSK) and will be discussed below.

2.4.1 Binary Phase Shift Keying

BPSK is accomplished by shifting the phase of the signal by 180 degrees depending on the sign of the data bit. For example, when the sign of the data bit in the message changes, the phase of the signal flips by 180 degrees. By doing so, only one bit can be modulated per symbol. GPS uses BPSK modulation for its CA codes, navigation data, and P(Y) codes (encrypted message). BPSK is used due to its resilience to bit error rate. A visual depiction of the BPSK signal can be seen in figure 2.5. In the figure, the phase change of the signal by 180 degrees can be seen at the change of each data bit.

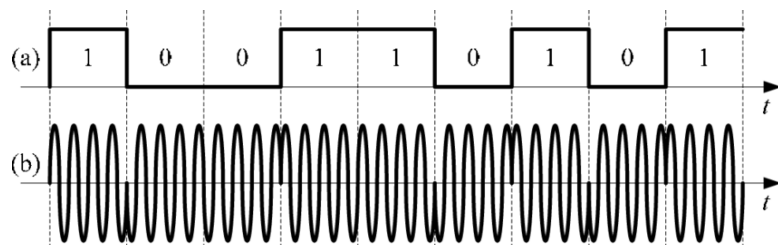


Figure 2.5: Binary Phase Shift Keying Visualization [3]

2.4.2 Quadrature Phase Shift Keying

QPSK modulation uses 4 possible phases of the signal to modulate the data onto the carrier wave. The phase possibilities are 90 degree offsets. With this, two bits are transmitted in one symbol. This allows for faster data rates of the signal. Figure 2.6 shows a visual example of QPSK modulation.

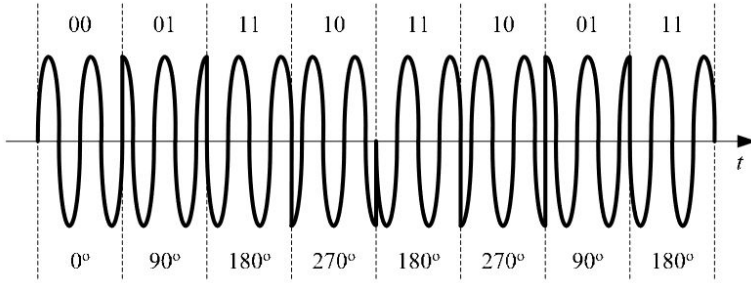


Figure 2.6: Quadrature Phase Shift Keying Visualization [3]

2.5 Satellite Based Navigation

Satellite navigation employs trilateration as a way to solve the age old problem of determining where ones self is on planet Earth. Trilateration is the process of using ranges to determine unknown locations of things. In a 2-dimentional example, three transmitters produce circles with radius r . With knowledge of the location of the transmitters, the ranges can be used to calculate a circle around the transmitter. The intersection point of all three circles will enclose the positioning result. This can be seen in figure 2.7.

The process of trilateration with satellites is the same except in 3-dimensional space. In the case of GPS, the satellites are the transmitters. Satellites make excellent transmitters in this case because of their ability to cover large areas continuously. An important point to mention is that in the previous example it is assumed that the satellite and receiver are tied to the same clock. This means that the user has a perfect known time of the transmission of the signal from the satellite and perfect knowledge of the time of reception. However, this is not the case in real world examples. In fact, each satellite is tied to its own clock while each receiver is also tied to a separate clock. This offset in time can cause very large errors in positioning.

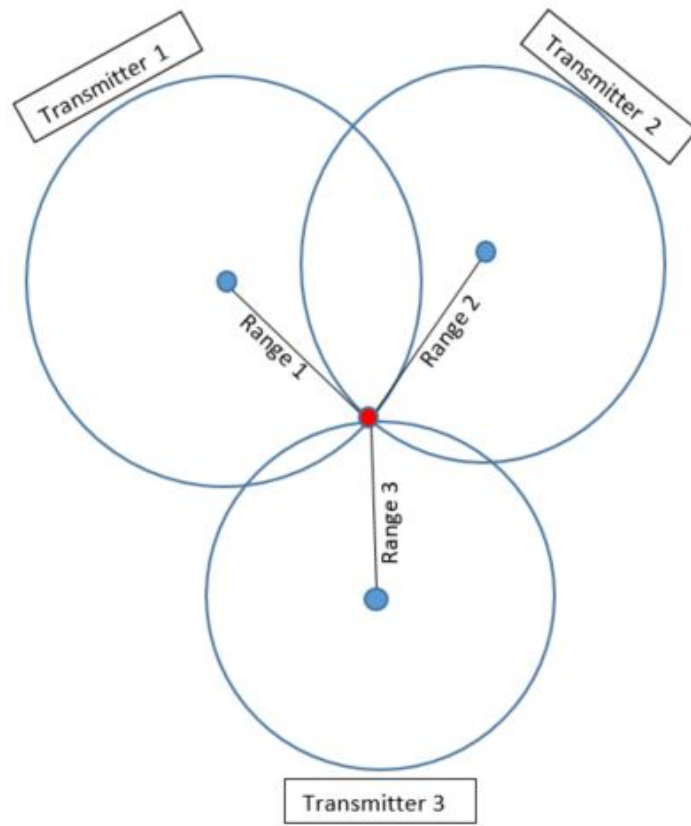


Figure 2.7: Visual Depiction of Trilateration

To account for this, GPS ground stations survey and monitor the status of the satellite clocks to ensure maximum clock accuracy. While this takes care of the satellite part of the clock issue, the receiver clock still contains error. This error can be estimated along with the receiver states with the addition of a fourth measurement.

Chapter 3

Simulation Tool

In this section, the function and versatility of the simulator will be described.

3.1 Simulator Overview

The overall structure of the simulation is shown in figure 3.1.

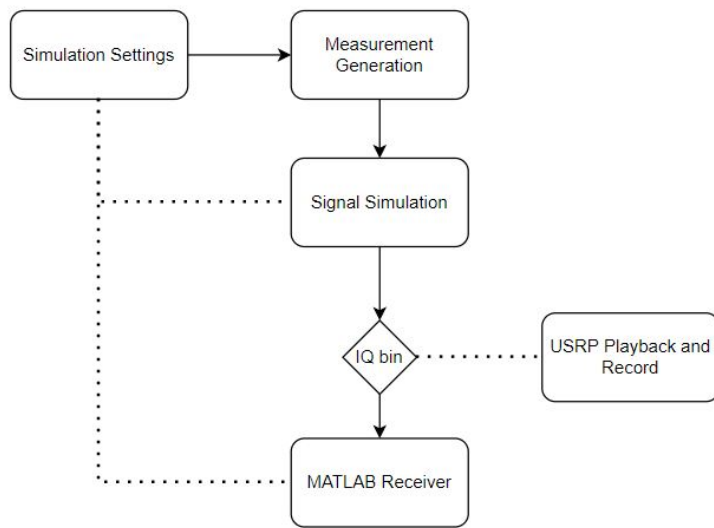


Figure 3.1: Overall Simulation Diagram

The simulation begins with the simulation settings file. This is a configuration file where all of the settings will be declared. This includes, but is not limited to, the satellite trajectories, signal power, and simulation length. The simulation settings file is fed into each block of the simulation tool. First, it goes into the measurement generation block. The measurement generation block is where the satellite positions and velocities are propagated, ranges and range

rates are calculated, and transmit and received times are produced. Those terms are pushed into the signal simulation. Inside the signal simulation block the signal is generated and packaged into a bin file. Finally, the bin file is sent to a receiver where it is picked up, processed, and decoded to produce measurements. The following subsections will address each part of the simulation.

3.2 Simulation Settings

The simulation settings is a configuration file where all of the constants and settings used throughout the simulation are declared. All of the settings are stored in a MATLAB structure labeled ‘settings’. A MATLAB structure is a data storing type where different variables can be tied to one overall variable. The purpose for incorporating all of the settings and variables in one script is to ensure all variables are in one place. This helps the user find a variable quickly and efficiently. It also aids the user by ensuring consistency across all parts of the simulation.

In part, the simulation settings allow this tool to be modular. The file begins with constants such as the speed of light, rotation rate of the Earth, Earth gravitational constants, and time constants. These will likely stay the same across any and all simulations. Next is the input of user time. This time is in the format of year, month, day, hour, minute, second and determines the start time of the simulation. Following the time starting point is the duration of the simulation in seconds and the measurement simulation sampling frequency in hertz. The next setting is the user position. Currently, the simulation allows for a static receiver with initial position defined in latitude, longitude, and altitude (LLA); however, the addition of a dynamic receiver can be made. Once the LLA position has been defined, the Earth centered Earth fixed (ECEF) position can be calculated. Next is the introduction of measurement error terms. The first set are weather terms for the error caused by the troposphere [4]. These inputs are temperature in Celsius and Kelvin, barometric pressure in millibars, and humidity as a percentage. This is followed by clock settings. Here the user declares what type of clock to use and whether the clock error is to be simulated, indicated by an on or off switch. The clock is modeled based on []. Next is the satellite propagation settings. This simulation uses a simplified general perturbation (SGP)

model for calculating satellite positions and velocities. Here the user will input a two line element (TLE) file name along with other information used in parsing the TLE. The propagation settings also includes a mask angle setting. The mask angle input is in degrees and allows the user to reject satellites under the specified elevation angle. After the satellite propagation settings are the signal settings. Here the user decides the carrier frequency, sampling frequency, code frequency, number of symbols in the data message, and signal type. One specific signal type is time division multiple access (TDMA). A TDMA signal uses time slots in the form of bursts to decipher different signals, whereas frequency division multiple access (FDMA) uses different frequency channels. If the declared signal type is TDMA, then the burst period will need to be calculated. This is followed by the noise and signal power.

The simulation settings file is integral to this simulation tool. All other components of this simulator are dependent on it. These specific dependencies will be explained in detail in the remaining subsections.

3.3 Measurement Simulation

The next block of the simulation tool is the measurement generation. The measurement generation is where the ranges, range rates, and times are calculated. The purpose of this section is to have a set of truth values that will be used later in the simulation. The block diagram for the measurement generation is shown in figure 3.2.

The measurement generation begins the same as all other blocks: inputting the simulation settings file. Again, this allows the user to have all of the same settings, constants, and configurations across all platforms. User positions are generated based on the initial input in the settings file. If a static receiver is declared, then the user position will remain the same and be populated at the set measurement sampling frequency. Along with the population of user positions, satellite positions and velocities are also propagated at this time. For this simulation, a simplified general perturbation (SGP) two line element (TLE) propagator is used to give truth values for satellite positions and velocities. The SGP4 TLE propagator outputs satellite positions and velocities in meters and meters per second, respectively, for the Earth centered

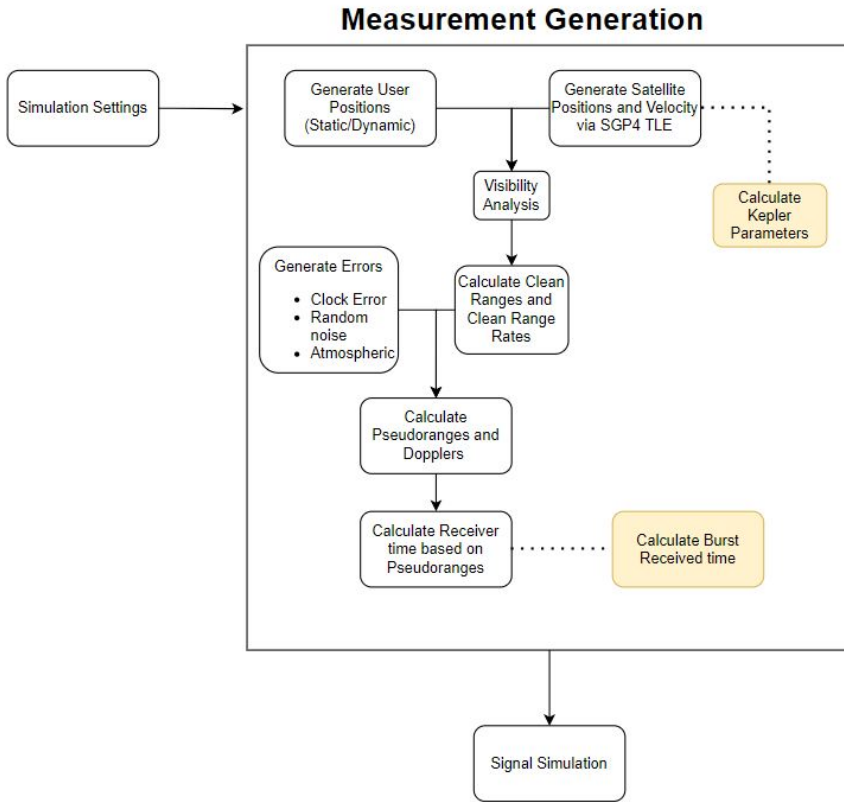
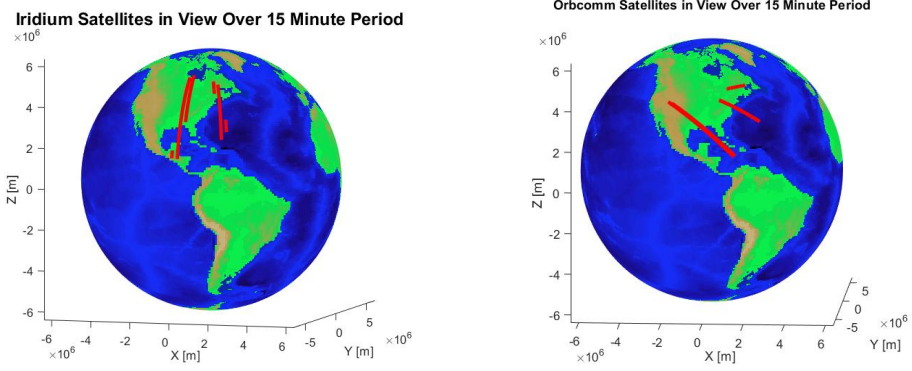


Figure 3.2: Measurement Generation Block Diagram

inertial (ECI) and ECEF coordinate frames. Figure 3.3 shows the propagated satellite orbits in view for the Iridium and Orbcomm constellations over the duration of the simulation.

With both the user position and satellite positions, a visibility analysis can be performed on the satellites. Another important output of the satellite propagation is the elevation angles of the satellites with respect to the user. The visibility analysis takes the elevation angles and finds the satellites that are above the mask angle to eliminate them from the simulation. The output of the visibility analysis is a list of satellites and the times that they are in view. This greatly reduces the computation time for the rest of the simulation because the simulator only has to compute values and signals for the specified satellites that are in view. An option the user has for a data message type is Kepler orbital parameters or classical orbital elements (COE). The calculation of COE uses the ECI satellite positions and velocities calculated previously. These terms are: h magnitude of angular momentum; e eccentricity; $RAAN$ right ascension of the ascending node, i inclination angle; w argument of perigee; TA true anomaly; a semi major axis. This process is described in. [26].



(a) Propagated Iridium Satellites in View (b) Propagated Orbcomm Satellites in View

Figure 3.3: Propagated Satellites from SGP4

After the visibility analysis, errors will be generated for the satellites that are in view. The first error generated is clock error. Clock bias and drift are generated for the receiver and the satellites. This option can be turned off and the errors will be incorporated as zeros in the simulation. Next the tropospheric delay is calculated from the settings defined previously. Finally, the addition of white Gaussian noise is added for errors not modeled (i.e. Ionosphere delay, multipath, etc). Simultaneously, the true satellite to receiver ranges are calculated along with the range rates. Their equations are show below.

$$r = \sqrt{(x_{sv}^{(k)} - x_u)^2 + (y_{sv}^{(k)} - y_u)^2 + (z_{sv}^{(k)} - z_u)^2} \quad (3.1)$$

$$\dot{r} = (\mathbf{v}^k - \mathbf{v}_r) \cdot \mathbf{\hat{1}} \quad (3.2)$$

Having generated ranges, range rates, and errors, the receiver observed pseudorange and Doppler measurements can be calculated. The equations for pseudorange, pseudorange rate, and Doppler are equations 3.3, 3.4, and 3.5, respectively.

$$\rho^{(k)} = r^{(k)} - b_{sv} + b_r + T + \epsilon \quad (3.3)$$

$$\dot{\rho} = \dot{r} + \dot{b}_r - \dot{b}_{sv} + \epsilon \quad (3.4)$$

$$f_{Doppler}^{(k)} = \frac{\dot{\rho}}{-\lambda} \quad (3.5)$$

Where in equation 3.3, ρ is the observed pseudorange calculated from range r to the k^{th} satellite, satellite clock bias b_{sv} , receiver clock bias b_r in meters, troposphere delay T , and additional noise for errors not modeled ϵ . In Equation 3.4, \dot{r} is the calculated range rate, \dot{b}_r is the receiver clock drift, \dot{b}_{sv} is the satellite clock drift, and un-modeled errors ϵ , all with units of meters per second. In equation 3.5, $f_{Doppler}^k$ is the Doppler frequency of the k^{th} satellite, $\dot{\rho}$ is the pseudorange rate, and λ is the wavelength of the carrier. Once the pseudorange and Doppler measurements have been calculated, the observed receive time of the signal can be calculated. It is important to calculate the received time of the signal based on the pseudorange because the signal is generated at the received level. The received time is calculated as

$$t_{rx} = t_{tx} + \frac{\rho}{c} \quad (3.6)$$

where t_{tx} is the transmit time, ρ is the pseudorange calculated in equation 3.3, and c is the speed of light. For a TDMA signal, burst timing needs to be calculated. For example, if the burst timing 70 milliseconds, then a burst will at $t = 0s$, $t = 0.07s$, $t = 0.14s$ and so on. For this instance, the received time of the signal is also calculated on the burst interval using equation 3.6.

The final outputs from the measurement generation are pseudoranges, Doppler Measurements, transmit times, received times, satellite positions, and satellite velocities. Classical orbital elements will be another output if the user has declared to use them for the navigation message. Once the measurements are calculated, the signal can be generated.

3.4 Signal Simulation

The signal simulation begins directly after the measurement generation. The current simulation is for a TDMA signal. The beginning of the simulation begins the transmission of a burst. Only

one burst occurs within the specified burst period. Figure 3.4 gives an overview of the signal simulation.

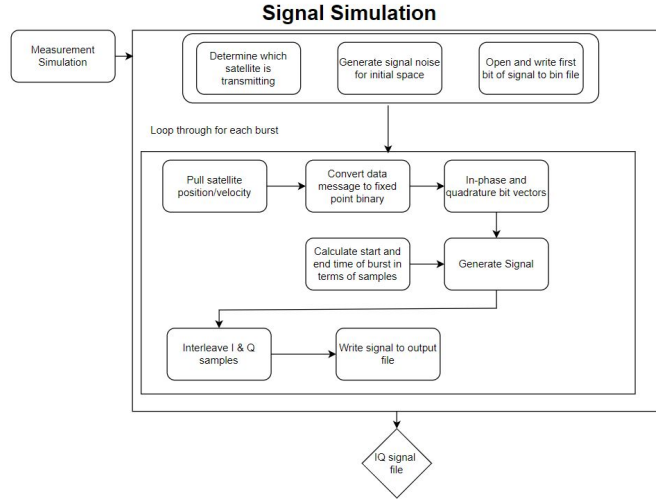


Figure 3.4: Signal Simulation Block Diagram

The simulation starts by determining what satellite is transmitting and stores it into an array. This process is probabilistic and one satellite in view is chosen at random to transmit. This process is performed for each burst at the start of the signal simulation. Once the burst transmission list has been determined, the first part of the signal is generated. The first part of the output file will be signal noise. The signal noise will be the length of the first transit time in terms of samples. For example, if the first transit time is 0.003009 seconds and the sampling frequency is one megahertz, the first 3009 samples will be noise. Next a bin file is generated and signal noise is written to the file.

With the calculated received times and designated satellites, we can generate the signal in blocks. We start by gathering the information for the data message. In this case, we gather satellite positions and velocities, satellite number, and transit time. Next, we convert those terms into fixed point binary strings. The data bits are generated in a separate function that is specific to the data message type. The length of each word is predetermined inside the data bit generation function. The fractional length is determined based on the amount of precision the user desires. The decision to sign the word is also declared. The outputs of the bit generation function are two row vectors of in-phase and quadrature bits. Non return to zero (NRZ) coding is used to represent the binary ones and zeros. The number of samples in the signal block is

determined by examining the begin time of the current burst and the begin time of the next burst. The difference in time is calculated and multiplied it by the signal sampling frequency in order to calculate the number of samples in the block. Next is the generation of the signal shown in figure 3.5.

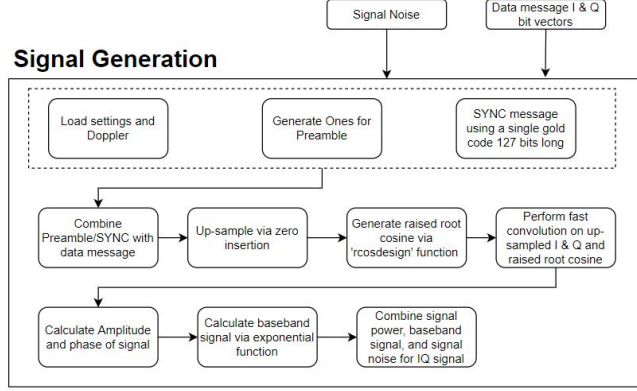


Figure 3.5: Signal Generation Block Diagram

A section of signal noise is generated for the amount of samples in the signal block. The signal noise and data message are input to the signal generation block. We start by loading in settings, Doppler frequency, preamble, and sync message. The sync message was chosen to be a 127 bit long gold code with an appended zero due to its autocorrelation abilities [27]. We then combine the preamble and sync messages on their respective branches along with the in-phase and quadrature bit vectors to produce our full data message. From there we up-sample via zero insertion and filtering with a root-raised-cosine (RRC) pulse shaping filter. The amplitude of the signal is calculated as equation 3.7 and the phase is calculated in equation 3.8

$$A = \sqrt{Ips^2 + Qps^2} \quad (3.7)$$

$$\theta = \tan^{-1} \frac{Qps}{Ips} \quad (3.8)$$

where Ips and Qps are the pulse shaped in-phase and quadrature branches respectively. The signal is generated through an exponential function in equation 3.9

$$Ae^{j2\pi(f_{Doppler}t+\theta)} \quad (3.9)$$

where A is the amplitude and θ is the phase. From here the declared signal power is added along side the signal noise. The output of the signal generation function is a full IQ signal with signal noise. The signal is then split into real and imaginary parts, where they are interleaved and written to the bin file. To save computational memory, the signal variables are cleared with each iteration. This process is performed for each block of signal throughout the simulation. At the end of the simulation, if there is a received time outside the bounds of the simulation time, then the simulation will end the file with signal noise.

3.5 Receiver

- Include stuff about burst receiver
 - Maximum likelihood burst detection - find source for this so I can talk about it in detail.
 - Decoding of the bits
 - Receiver outputs. Decoded Navigation Message, Doppler Frequency, location of the bit (to get a range), Failed bursts, Successful Bursts, output bits for bit error calculation,

Chapter 4

Testing Setup and Positioning Techniques

This chapter will discuss positioning techniques used for validation of results in this thesis. Two specific positioning techniques are Doppler based and Pseudorange based. These techniques will be used along with the outputs of the receiver in order to gain a positioning solution.

4.1 Doppler Based Positioning

Doppler positioning is not a new technique. In fact it was used with the original TRANSIT system in the 1960's and positioning accuracy was found to be within 500 meters. Doppler shift occurs as a result of a transmitter moving relative to an observer. As the transmitter moves closer, the frequency of the signal increases as the wave is being pushed closer to the observer. The opposite is true as the transmitter moves away from the user. The basis of Doppler positioning is using the change in signal frequency to gain an understanding of the motion of the transmitter. That information along with known satellite states can be used to gain a positioning solution.

The outputs of the receiver detailed in this thesis include the satellite position vector \mathbf{r}_{sv} , the satellite velocity vector \mathbf{v}_{sv} and the received Doppler frequency $f_{Doppler}$. By rearranging 3.5, the pseudorange rate of the k^{th} satellite can be calculated in 4.1.

$$\dot{\rho}^k = f_{Doppler}^k \cdot -\lambda \quad (4.1)$$

Using 4.1 and 3.2 to rearrange 3.4, the following equation is developed.

$$\dot{\rho}^k = (\mathbf{v}^k - \mathbf{v}_u) \cdot \frac{(\mathbf{x}^k - \mathbf{x}_u)}{\|\mathbf{x}^k - \mathbf{x}_u\|} + \dot{b} + \epsilon^k \quad (4.2)$$

For a static receiver \mathbf{v}_u in equation 4.2 will be zero resulting in equation 4.3.

$$\dot{\rho}^k = \mathbf{v}^k \cdot \frac{(\mathbf{x}^k - \mathbf{x}_u)}{\|\mathbf{x}^k - \mathbf{x}_u\|} + \dot{b} + \epsilon^k \quad (4.3)$$

With knowledge of the satellite states from the decoded navigation message, the unknowns are \mathbf{x}_u and \dot{b} , where

$$\mathbf{x}_u = \begin{bmatrix} x_u \\ y_u \\ z_u \end{bmatrix}. \quad (4.4)$$

With four unknowns, at least four measurements will be needed to solve for a positioning solution. An iterative process can be used to solve for the unknowns. First, an initial estimate of the states must be made. This will be represented by

$$\hat{\mathbf{x}} = \begin{bmatrix} \hat{x}_u \\ \hat{y}_u \\ \hat{z}_u \\ \hat{b} \end{bmatrix} \quad (4.5)$$

where the \mathbf{x} is the vector of all unknown states, including the clock term. Next is a vector of pseudorange rate measurements from 4.1 taking the form

$$\dot{\rho} = \begin{bmatrix} \dot{\rho}_1 \\ \dot{\rho}_2 \\ \vdots \\ \dot{\rho}_n \end{bmatrix} \quad (4.6)$$

where n is the number of measurements being used. Next an estimate of the pseudorange rate is calculated for each satellite by combining 4.5 and 4.3 to form

$$\hat{\dot{\rho}} = \begin{bmatrix} \mathbf{v}_1 \cdot \frac{(\mathbf{x}_1 - \hat{\mathbf{x}}_u)}{\|\mathbf{x}_1 - \hat{\mathbf{x}}_u\|} + \hat{b} \\ \mathbf{v}_2 \cdot \frac{(\mathbf{x}_2 - \hat{\mathbf{x}}_u)}{\|\mathbf{x}_2 - \hat{\mathbf{x}}_u\|} + \hat{b} \\ \vdots \\ \mathbf{v}_n \cdot \frac{(\mathbf{x}_n - \hat{\mathbf{x}}_u)}{\|\mathbf{x}_n - \hat{\mathbf{x}}_u\|} + \hat{b} \end{bmatrix} \quad (4.7)$$

The measurement matrix $\mathbf{H}(\hat{\mathbf{x}})$ takes the form below where it is an $n \times 4$ matrix, where n is the number of measurements being used.

$$\mathbf{H}(\hat{\mathbf{x}}) = \begin{bmatrix} \frac{(\mathbf{x}_1 - \hat{\mathbf{x}}_u)}{\|\mathbf{x}_1 - \hat{\mathbf{x}}_u\|} \times \left(\frac{(\mathbf{x}_1 - \hat{\mathbf{x}}_u)}{\|\mathbf{x}_1 - \hat{\mathbf{x}}_u\|} \times \frac{\mathbf{v}_1}{\|\mathbf{x}_1 - \hat{\mathbf{x}}_u\|} \right) & 1 \\ \frac{(\mathbf{x}_2 - \hat{\mathbf{x}}_u)}{\|\mathbf{x}_2 - \hat{\mathbf{x}}_u\|} \times \left(\frac{(\mathbf{x}_2 - \hat{\mathbf{x}}_u)}{\|\mathbf{x}_2 - \hat{\mathbf{x}}_u\|} \times \frac{\mathbf{v}_2}{\|\mathbf{x}_2 - \hat{\mathbf{x}}_u\|} \right) & 1 \\ \vdots & \vdots \\ \frac{(\mathbf{x}_n - \hat{\mathbf{x}}_u)}{\|\mathbf{x}_n - \hat{\mathbf{x}}_u\|} \times \left(\frac{(\mathbf{x}_n - \hat{\mathbf{x}}_u)}{\|\mathbf{x}_n - \hat{\mathbf{x}}_u\|} \times \frac{\mathbf{v}_n}{\|\mathbf{x}_n - \hat{\mathbf{x}}_u\|} \right) & 1 \end{bmatrix} \quad (4.8)$$

With this form, an estimate of the position and clock drift can be calculated using an iterative process. The first step of the process is to fill in equation 4.8 with the initial guess position guess, satellite positions, satellite velocities. The next process is to calculate the pseudorange rates using 4.7. The next process is to create a delta pseudorange rate using equation 4.9.

$$\delta\dot{\rho} = \dot{\rho} - \hat{\dot{\rho}} \quad (4.9)$$

By using the delta pseudorange rate, the error of the original estimate is what is being calculated. This is calculated through least squares shown in equation 4.10.

$$\tilde{\mathbf{x}} = (\mathbf{H}^T \mathbf{H})^T \mathbf{H}^T \delta\dot{\rho} \quad (4.10)$$

The new position estimate is calculated through 4.11.

$$\hat{\mathbf{x}}_{\text{new}} = \hat{\mathbf{x}}_{\text{old}} + \tilde{\mathbf{x}} \quad (4.11)$$

This process is continued iteratively until some threshold is met. Once the threshold is met, the process is concluded and the position and clock drift are output.

This process is typically employed using four or more measurements at the same time. For this thesis, a batched technique will be used. Since the nature of the signal used in this thesis is discontinuous, only one measurement is received at each time. One way to combat this is to use batched measurements. Batching measurements means taking measurements over a select period of time and treating them as if they all have come at one time. The advantage of batching measurements is that it allows the user to have enough measurements to gain an accurate position. Typically, when batching measurements, many measurements must be used in order to gain geometric diversity apart from each other. One disadvantage of batching measurements is that it can take longer periods of time to gather enough measurements in order to gain a position estimate. Long term, the act of batching measurements is similar to averaging them all over time.

4.2 Pseudorange Based Positioning

Pseudorange based positioning is also not a new concept. Pseudoranges are used to solve the trilateration problem discussed in section 2.5. Equation 3.3 previously discussed is the pseudorange equation. It includes the true range, satellite and receiver clock errors, atmospheric errors, and unmodeled effects. Similar to the Doppler positioning in section 4.1, an iterative process is used to solve for a positioning solution. However instead of using the range rate, the pseudorange is used. There are a few modifications that need to be made to the equations used in this process, however the process of solving for the position as a whole is quite similar.

- - Mention things about the configuration:
- - satellite orbits
- - signal type
- - USRP playback and record
- - why important
- - how it works

- - how USRPs work in brief

Chapter 5

Results

This chapter will be used to show the results from simulations run in this thesis. The purpose of these results is to show that the simulation tool is capable of producing a signal that gives realistic results.

5.1 Static Clean Data

The data set generated for this scenario is a static data set with zero clock error, zero thermal signal noise, and zero atmospheric errors. The purpose of this experiment was to examine what the cleanest possible data set would produce.

5.1.1 Doppler Positioning

The first positioning strategy for this data set is using the received Doppler measurements in a batched fashion using the equations in section 4.1.

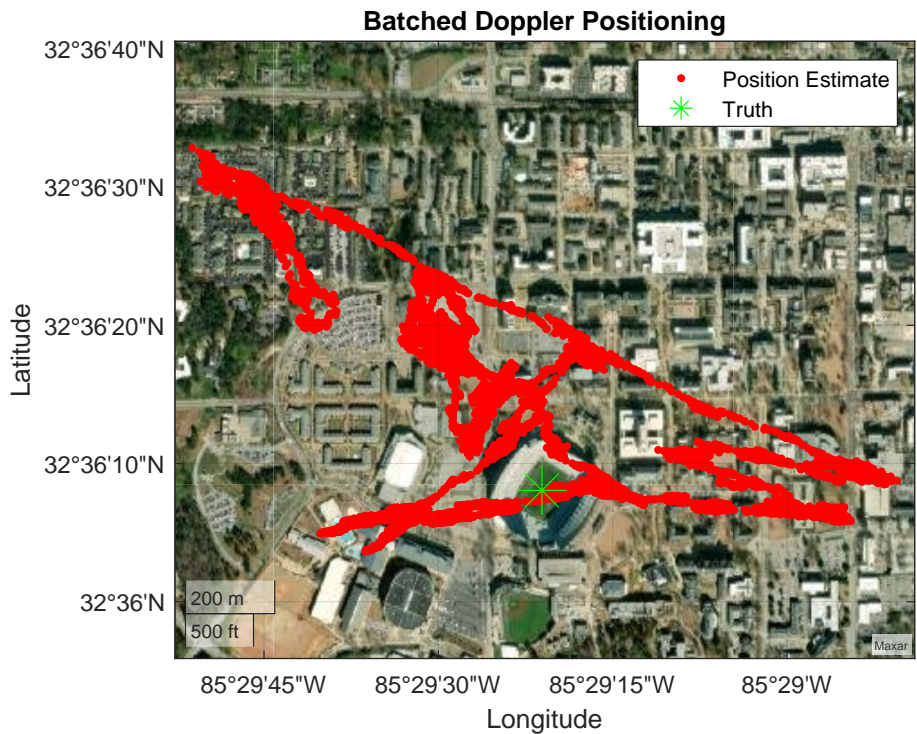


Figure 5.1: Position Estimate from Batched Doppler Measurements

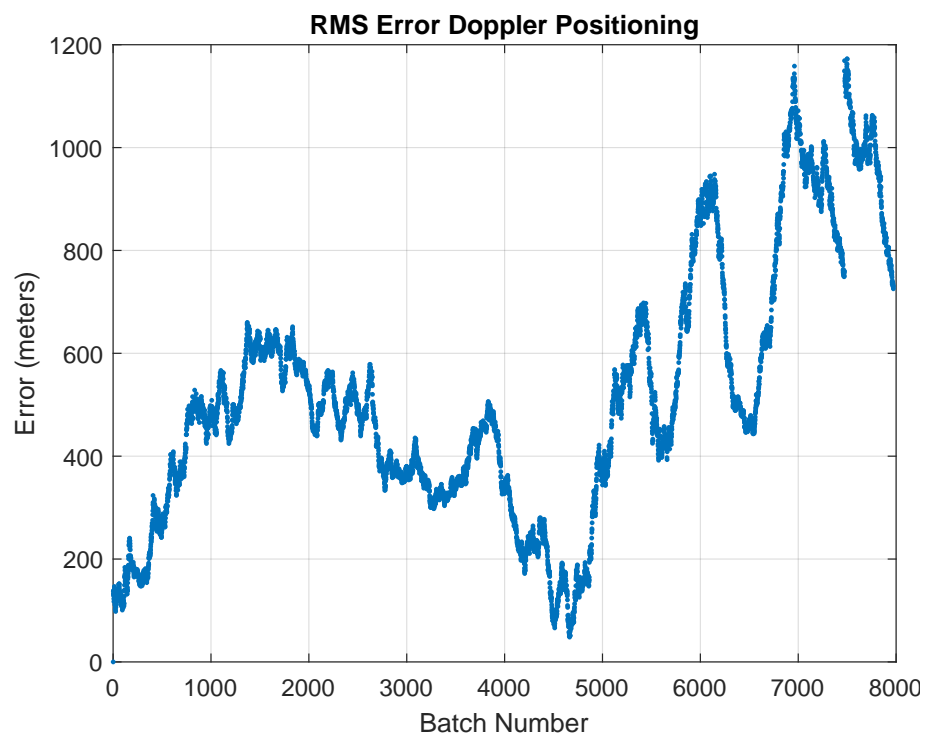


Figure 5.2: RMS Error of Batched Doppler Estimates

5.1.2 Pseudorange Based Positioning

5.2 Static Clean Data Played Through USRP

5.2.1 Doppler Positioning

5.2.2 Pseudorange Based Positioning

5.3 Static Dirty Data

5.3.1 Doppler Positioning

5.3.2 Pseudorange Based Positioning

5.4 Dynamic Clean Data

5.5 Dynamic Clean Data Played Through USRP

5.6 Dynamic Dirty Data

- positioning results

- Doppler Positioning
- comparison of constellations
- positioning algorithms
- batch recursive least squares
- 2d positioning and 3d positioning
- possible aided doppler positioning techniques
- How many bursts were detected and accurately decoded
- Possible testing configurations
- Full clean data (no clock, no noise, no trop)
- Full clean data run through USRP
- Simulated dirty set with trop error, clock error, sig noise
- Run this simulation for 2 different satellite constellations
- See if I have to run it for a dynamic rover - Update:I do.

Chapter 6

Conclusions and Future Work

- The simulator works well
 - addition of more signals
 - addition of multiple constellation
 - addition of more error terms

Bibliography

- [1] Amplitude Shift Keying.
- [2] Frequency Shift Keying.
- [3] Ghafour Amouzad Mahdiraji and Ahmad Fauzi Abas. Advanced Modulation Formats and Multiplexing Techniques for Optical Telecommunication Systems. March 2010.
- [4] Pratap Misra and Per Enge. *Global Positioning System; Signals, Measurements, and Performance*. Ganga-Jamuna Press, Lincoln, Massachusetts, revised second edition edition, 2012.
- [5] Lei Dong. *IF GPS Signal Simulator Development and Verification*. PhD thesis, University of Calgary, Alberta, Calgary, Canada, November 2003.
- [6] Phillip Martin Corbell. *Design and Validation of an Accurate GPS Signal and Receiver Truth Model for Comparing Advanced receiver Processing Techniques*. PhD thesis, Air Force Institute of Technology, Wright-Patterson Air Force Base, Ohio, March 2000.
- [7] Russell Powell. *A Multiple-Antenna Software GPS Signal Simulator forRapid Testing of Interference Mitigation Techniques*. PhD thesis.
- [8] Wu-Hung Hsu and Shau-Shiun Jan. Assessment of using Doppler shift of LEO satellites to aid GPS positioning. In *2014 IEEE/ION Position, Location and Navigation Symposium - PLANS 2014*, pages 1155–1161, Monterey, CA, USA, May 2014. IEEE.
- [9] Mark L. Psiaki. Navigation using carrier Doppler shift from a LEO constellation: TRAN-SIT on steroids. *NAVIGATION*, 68(3):621–641, September 2021.

- [10] Mojtaba Bahrami. GNSS Doppler Positioning (An Overview). page 17.
- [11] Transit Satellite: Space-based Navigation.
- [12] Sterling Thompson. Single Differenced Doppler Positioning with Low Earth Orbit Signals of Opportunity and Angle of Arival Estimation. In *Proceedings of the 2021 International Technical Meeting*, pages 497–509, Long Beach, CA, January 2021.
- [13] Remy Lopez, Jean-Pierre Malarde, Francois Royer, and Philippe Gaspar. Improving Argos Doppler Location Using Multiple-Model Kalman Filtering. *IEEE Transactions on Geoscience and Remote Sensing*, 52(8):4744–4755, August 2014.
- [14] Joe J. Khalife and Zaher M. Kassas. Receiver Design for Doppler Positioning with Leo Satellites. In *ICASSP 2019 - 2019 IEEE International Conference on Acoustics, Speech and Signal Processing (ICASSP)*, pages 5506–5510, May 2019. ISSN: 2379-190X.
- [15] Zizhong Tan, Honglei Qin, Li Cong, and Chao Zhao. New Method for Positioning Using IRIDIUM Satellite Signals of Opportunity. *IEEE Access*, PP:1–1, June 2019.
- [16] Joshua J. Morales, Joe Khalife, Ali A. Abdallah, Christian T. Ardito, and Zak M. Kassas. Inertial Navigation System Aiding with Orbcomm LEO Satellite Doppler Measurements. pages 2718–2725, Miami, Florida, October 2018.
- [17] Tyler G.R. Reid, Bryan Chan, Ashish Goel, Kazuma Gunning, Brian Manning, Jerami Martin, Andrew Neish, Adrien Perkins, and Paul Tarantino. Satellite Navigation for the Age of Autonomy. In *2020 IEEE/ION Position, Location and Navigation Symposium (PLANS)*, pages 342–352, April 2020. ISSN: 2153-3598.
- [18] NOAA US Department of Commerce. Satellites. Publisher: NOAA’s National Weather Service.
- [19] Rob Garner. GOES Overview and History, March 2015.
- [20] GLONASS Interface Control Document. page 47, 1998.

- [21] Mohamad Orabi, Joe Khalife, and Zak Kassas. Opportunistic Navigation with Doppler Measurements from Iridium Next and Orbcomm LEO Satellites. April 2021.
- [22] Iridium NEXT: In Review, February 2019.
- [23] Starlink.
- [24] R. Gold. Optimal binary sequences for spread spectrum multiplexing (Corresp.). *IEEE Transactions on Information Theory*, 13(4):619–621, October 1967. Conference Name: IEEE Transactions on Information Theory.
- [25] GLONASS Signal Plan - Navipedia.
- [26] Howard D. Curtis. *Orbital mechanics for engineering students*. Elsevier Aerospace engineering series. Elsevier Butterworth Heinemann, Amsterdam Heidelberg, 1. ed., reprinted edition, 2008.
- [27] E.H. Dinan and B. Jabbari. Spreading codes for direct sequence CDMA and wideband CDMA cellular networks. *IEEE Communications Magazine*, 36(9):48–54, September 1998. Conference Name: IEEE Communications Magazine.

Appendices